RESEARCH ARTICLE

Inactivation effect and mechanisms of combined ultraviolet and metal-doped nano-TiO$_2$ on treating *Escherichia coli* and *Enterococci* in ballast water

Xixi Wang[1] · Yanli Huang[1] · Kun Zhang[1] · Yue Shi[1] · Zheng Lu[1] · Yinhao Wang[1]

Abstract

The discharge of ship ballast water (containing large amounts of alien organisms) has caused severe ecological hazards to marine environments. In this study, three metal elements (Ag, Fe, and Gd) were doped to nano-TiO$_2$ material respectively (content: 0.4%, 0.7%, and 1.0%) to improve inactivation effect of *Escherichia coli* and *Enterococci* in ballast water. Experimental results indicate that compared with the sole ultraviolet (UV) and the UV and original nano-TiO$_2$, the UV and metal-doped nano-TiO$_2$ increased the bacterial inactivation rate to different extents. For each metal element, high external metal content (1.0%) corresponded to high inactivation effort. The doping of Ag resulted in optimal inactivation effort, and the addition of Fe and Gd caused unobvious effort. At the end of the inactivation process (20 s), the UV and 1% Ag-doped nano-TiO$_2$ reached the highest logarithmic sterilization rates (0.915 for *Escherichia coli* and 0.805 for *Enterococcus*). The doping of Ag, Fe, and Gd did not change the anatase phase TiO$_2$ crystal form, and 1% Ag-doped nano-TiO$_2$ had the smallest particle diameter and the evenest distribution of nanoparticles. Compared with the sole UV, the UV and Ag-doped nano-TiO$_2$ treatment resulted in higher malondialdehyde contents (0.0646 μmol/L for *Escherichia coli* and 0.0529 μmol/L for *Enterococci*) and lower superoxide dismutase activities (0.672 U/mL for *Escherichia coli* and 0.792 U/mL for *Enterococci*), which were in accordance with high inactivation rates in these cases.

Keywords Ship ballast water · Metal-doped nano-TiO$_2$ · Inactivation · Material characteristics · Malondialdehyde (MDA) · Superoxide dismutase (SOD)

Introduction

With the prosperity of shipping industry, the discharge of ship ballast water has become a serious threat to marine ecological environment. It is estimated that about 10 billion tons of ballast water are transferred worldwide each year, resulting in unexpected introduction of non-indigenous organisms to their new habitat. Once the alien organisms (such as microalgae and bacteria) adapt to the new environmental conditions, their proliferation might lead to severe ecological disaster, such as algal blooms. In addition, many researches indicated that heterotrophic microorganisms (bacteria, viruses, etc.) could be introduced into uncontaminated areas by ship ballast water, posing a potential hazard to human health (Leichsenring and Lawrence 2011; Seiden et al. 2010). The International Maritime Organization (IMO) has set stringent standards on living bacteria in discharged ballast water (*Escherichia coli*: < 250 cfu/100 mL; *Enterococci*: < 100 cfu/100 mL), and the development of efficient bacterial inactivation techniques has become a hot spot in the field (Tao et al. 2017).

Generally, ship ballast water treatment system is composed of a filtration unit and an inactivation unit. Since the main effort of the filtration unit is to keep out large planktons, bacterial inactivation is mainly achieved in the inactivation unit (Tang et al. 2009; Tsolaki and Diamadopoulos 2010). Among various disinfection methods, ultraviolet (UV) radiation is considered a favorable method with its significant advantages of simple unit configuration, high adaptability under different

---

✉ Kun Zhang
  kunzhang@hrbeu.edu.cn

✉ Yue Shi
  shiyue@hrbeu.edu.cn

[1] College of Power and Energy Engineering, Harbin Engineering University, Harbin 150001, China

salinities, none of corrosion to pipelines, and no harmful oxidant substances production (Mamlook et al. 2008). However, the inactivation effect of the UV radiation can be greatly limited at high seawater turbidities, and bacteria can survive the UV treatment due to the effect of photoreactivation and dark repair. Recently, combined UV and nano-TiO_2 photocatalysis technology has caught much sight to inhibit the photoreactivation and dark repair of bacteria (Shang et al. 2009). Under UV irradiation, nano-TiO_2 catalyst can generate a large number of reactive oxygenated species, which are highly effective to deconstruct cellular structure, accelerate the death of microorganisms, and prevent the regeneration of harmful microorganisms in the ballast water (Martínez et al. 2013).

The combined UV and nano-TiO_2 technology has proven an efficient disinfection alternative for ballast water treatment (Roy et al. 2018), and its restrictions mainly lie in the inherent characteristics of nano-TiO_2. For instance, TiO_2 has a large band gap energy (3.2 eV for anatase phase and 3.0 eV for rutile phase), and the spectral response range is narrow. In order to improve material properties, the modification of nano-TiO_2 by doping other elements has attracted much attention (Banerjee et al. 2016). By doing this, the separation probability of electrons and holes can be increased, and the recombination of electron-hole pairs can be inhibited, resulting in improved photocatalytic performance of nano-TiO_2. Some kinds of elements have been investigated, such as Au (Radzig et al. 2019; Veziroglu et al. 2018), Ag (Rtimi et al. 2019), Cu (Wu et al. 2018), Co (Smirnova et al. 2017), Fe (Mangayayam et al. 2017; Yu et al. 2019), and nonmetal elements such as F and N (Makropoulou et al. 2018; Milosevic et al. 2017). However, while using the combined UV and metal-doped nano-TiO_2 technology, the effect of doping elements (type and ratio) on bacterial inactivation was less investigated, and there is still a lack of knowledge on bacterial inactivation mechanisms.

In our previous researches, the inactivation effect of UV-TiO_2 on microalgae and *Escherichia coli* has been investigated, and the results proved the effectiveness of the UV-TiO_2 technique on treating ballast water containing high contents of suspended matter (Lu et al. 2018, Lu et al. 2019). In this study, three representative metal elements (Ag, Fe, and Gd) were doped to nano-TiO_2 at different ratios (0.4%, 0.7%, and 1.0%) to generate metal-doped nano-TiO_2 materials. The inactivation effect of sole UV, UV and nano-TiO_2, and UV and metal-doped nano-TiO_2 was compared with *Escherichia coli* and *Enterococci* as the inactivation objects. The prepared metal-doped nano-TiO_2 materials were characterized by scanning electron microscope (SEM), X-ray diffraction (XRD), and X-ray energy dispersive spectroscopy (EDS). Malondialdehyde (MDA) concentration and superoxide dismutase (SOD) activity were analyzed to reveal bacterial inactivation mechanisms of the combined UV and metal-doped nano-TiO_2 technology.

Materials and methods

Artificial ballast water and bacterial cultivation

Artificial ballast water was prepared according to Mocledon's artificial seawater formula. The 200-mesh calcium-based organic bentonite was supplemented as an additive to make the ballast water having a turbidity of 10 NTU. The pH of the artificial ballast water was adjusted to 8.0. As the inactivation objects, *Escherichia coli* and *Enterococcus* were purchased from China General Microbiological Culture Collection Center (CGMCC). Prior to the inactivation process, the two kinds of bacteria were inoculated in autoclaved Luria broth liquid medium. The bacterial culture was carried out in an incubator at 37 °C for 18–24 h and then ready for the following inactivation experiments.

Preparation of original and metal-doped nano-TiO_2

The original and metal-doped nano-TiO_2 were prepared by the sol-gel method (Yang et al. 2018). The procedures were as follows: 10 mL tetrabutyl titanate solution was slowly added into 35 mL anhydrous ethanol. The mixture was thoroughly agitated for 10 min by using a magnetic stirrer, generating solution A. In addition, 35 mL anhydrous ethanol, 4.08 mL deionized water, and 4.08 mL glacial acetic were mixed and supplemented with nothing (for preparing original nano-TiO_2), silver nitrate (for doping Ag), ferric nitrate nonahydrate (for doping Fe), and gadolinium nitrate hexahydrate (for doping Gd), respectively. For each doped metal element, the doping ratio was 0.4%, 0.7%, and 1.0%, respectively. The mixture was named solution B, and its pH was adjusted to less than 3.0 by using nitric acid. Afterwards, while the solution B was heated and stirred in a water bath at 30 °C, the solution A was slowly added into the solution B at a speed of one drop per second. After the stirring of 1 h, the mixture was called solution C. The catalyst in the solution C was loaded on the pretreated nickel foam by using a dip coater, and the loading times were fifteen. After that, the loaded nickel foam was dried at 80 °C for 10 min, put into a muffle furnace at 445 °C for 2 h, and then insulated for 12 h. The original and metal-doped nano-TiO_2 were then prepared for the further use.

Inactivation device and operation process

An inactivation device was designed to explore inactivation effect and mechanisms of *Escherichia coli* and *Enterococcus* using sole UV, UV and nano-TiO_2, and UV and metal-doping nano-TiO_2. Figure 1 displays the schematic diagram of the inactivation device, which was mainly composed of a UV lamp, a light shielding plate, a glass reaction vessel (containing bacterial suspension diluted from the cultural solution),

Fig. 1 Schematic diagram of the inactivation device
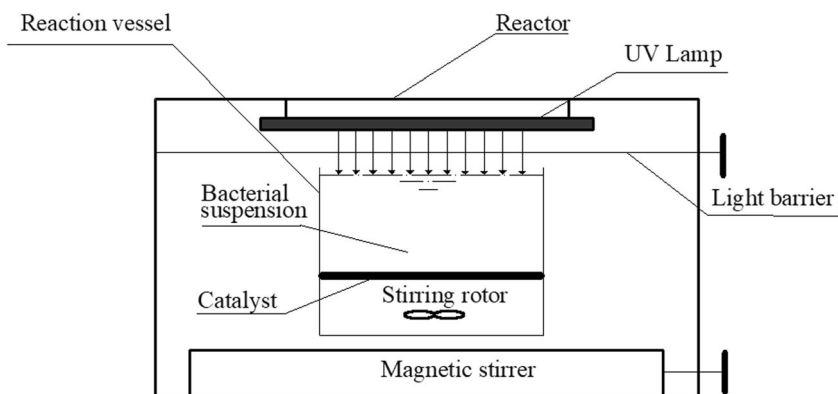
and a magnetic agitator. Before the inactivation process, the UV lamp was preheated for 15 min to obtain a stable UV light intensity. *Escherichia coli* and *Enterococcus* were separately used as the inactivated object with an initial concentration of about 10^4 cfu/mL. The device was operated for inactivating the two bacterial suspensions using the sole UV treatment, the combined UV and original nano-TiO_2 treatment, and the combined UV and metal-doped nano-TiO_2 treatment, respectively. During the treatment process (0 s, 5 s, 10 s, 15 s, and 20 s), bacterial suspension was obtained to analyze the number of living bacteria. In addition, a continuous flow device was used to analyze MDA content and SOD activity as previously described (Lu et al. 2018). For each trial, three parallel samples were analyzed to make sure the data reproducibility. All experiments were carried out at a room temperature of 22 °C.

Inactivation rate of *Escherichia coli* and *Enterococcus*

Escherichia coli and *Enterococcus* were numbered according to the following procedures. The bacterial suspension was proportionately diluted and then filtered by a vacuum pump. Bacteria were then entrapped by the membrane, and the membrane was attached to the surface of the Luria broth solid medium for further cultivation (37 ± 0.5 °C for 24 ± 1 h). Afterwards, the number of colonies was counted to calculate bacterial concentrations in the suspension. The logarithmic sterilization rate (η) was used to reflect the inactivation rate of bacteria in the device, and the calculation formula is $\eta = - \lg(N_t/N_0)$, where N_0 is the number of living bacteria before the inactivation treatment and N_t is the number of bacteria in the sample at different treatment times.

Materials characterization

The microstructure and morphology of the prepared materials (original nano-TiO_2 and metal-doped nano-TiO_2) were analyzed using SEM (Quanta 200, FEI, Netherlands), and the EDS analysis of the materials was

performed by using an energy dispersive spectrometer (TEAM™, EDAX, USA). The crystal structure of the
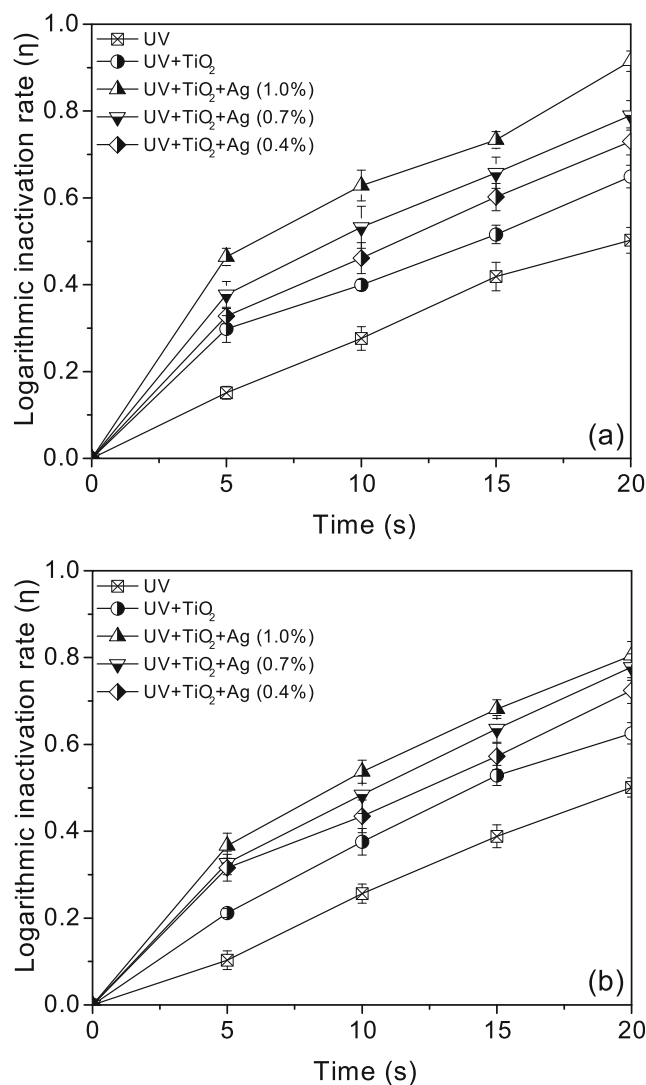
Fig. 2 Logarithmic sterilization rate for the sole UV, the UV and original nano-TiO_2, and the UV and Ag-doped nano-TiO_2 treatment. **a** *Escherichia coli* and **b** *Enterococci*

materials was analyzed by an XRD analyzer (D/max 2550 VB⁺, Rigaku, Japan). The radiation source was Cu Kα ($\lambda = 0.15406$ nm), the scanning range was 10–80°, the tube voltage was 40 kV, the current used was 30 mA, and the scanning speed was 5°/min. The average crystallite size D was calculated by the Scherrer formula $D = K\gamma/(B\cos\theta)$, where D is the average thickness of the grain perpendicular to the crystal plane direction, K is the Scherrer constant, γ is the X-ray wavelength, which is 0.154056 nm, B is the half-height width of the diffraction peak of the measured sample, and θ is the diffraction angle.

## Measurement of MDA content and SOD activity

As an important indicator reflecting cell membrane damage, MDA content was measured using the thiobarbituric acid method (Esterbauer 1996). With the capability of eliminating harmful substances produced by cell metabolism, the activity of SOD was analyzed using the pyrogallol method (Marklund et al. 1974). The detailed analytical procedures of MDA content and SOD activity were in accordance with the previous studies.
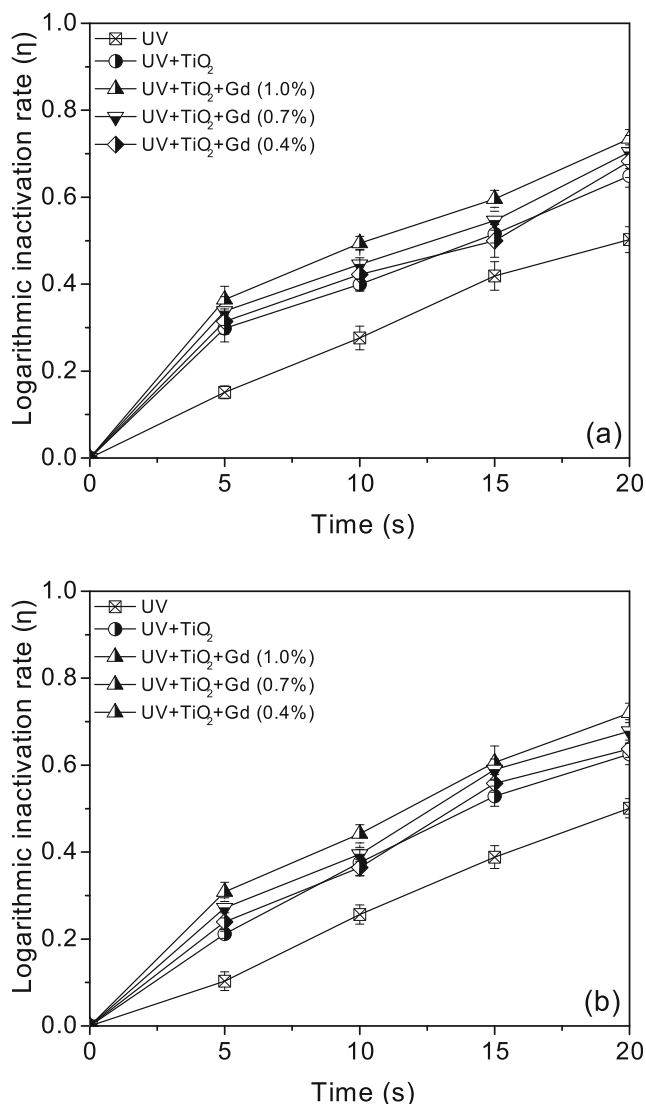
Results and discussion

Inactivation effect of the combined UV and Ag, Fe, and Gd-doped nano-TiO₂

The inactivation effect of the combined UV and Ag, Fe, and Gd-doped nano-TiO₂ was investigated with
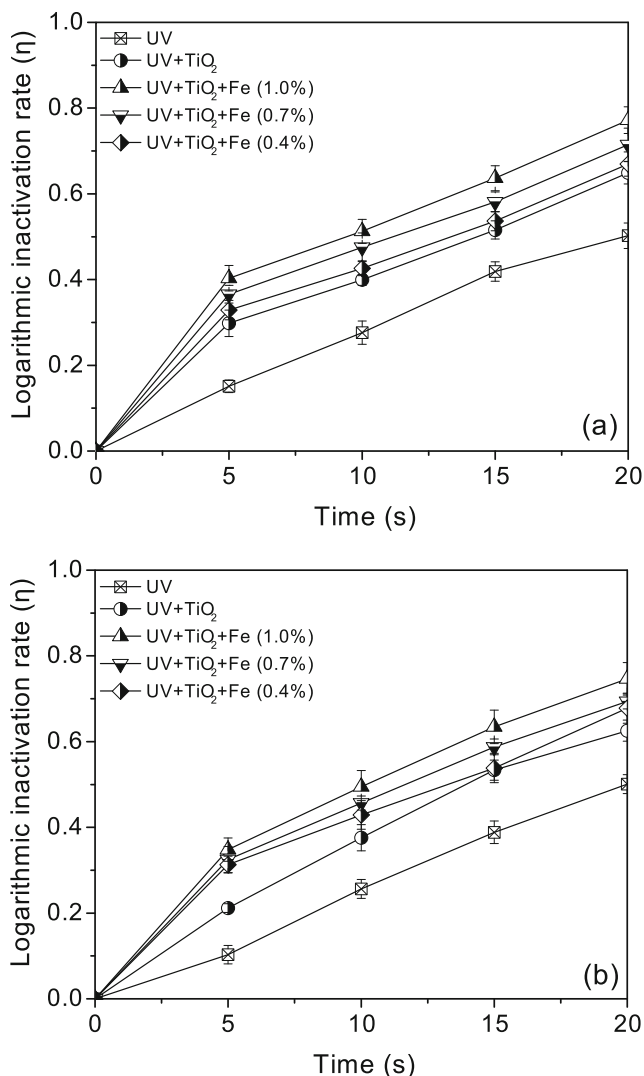
Fig. 3 Logarithmic sterilization rate for the sole UV, the UV and original nano-TiO₂, and the UV and Fe-doped nano-TiO₂ treatment. **a** *Escherichia coli* and **b** *Enterococci*


Fig. 4 Logarithmic sterilization rate for the sole UV, the UV and original nano-TiO₂, and the UV and Gd-doped nano-TiO₂ treatment. **a** *Escherichia coli* and **b** *Enterococci*

Escherichia coli and *Enterococcus* as the inactivation objects. Figure 2 shows the logarithmic sterilization rates of the UV and Ag-doped nano-TiO$_2$ treatment. Compared with the sole UV and the UV and nano-TiO$_2$ treatment, the doping of Ag significantly improved the inactivation effect on the two kinds of typical bacteria. Within the Ag content range in this study, the higher the Ag content in the nano-TiO$_2$ material was, the higher the inactivation rates of the two bacteria were. With the doping of 1% Ag, the logarithmic sterilization rates of *Escherichia coli* and *Enterococcus* reached 0.915 and 0.805, respectively, at the end, which were 0.266 and 0.179 higher than those of the UV and nano-TiO$_2$ treatment. Figure 3 displays the logarithmic sterilization rates while using the UV and Fe-doped nano-TiO$_2$. It indicates that the doping of Fe slightly increased the inactivation effect of *Escherichia coli* and *Enterococcus*. The doping of 1% Fe reached the optimal logarithmic sterilization rates (0.772 for *Escherichia coli* and 0.746 for *Enterococcus*), which were 0.123 and 0.120 higher than those of the UV and nano-TiO$_2$ treatment, respectively. The logarithmic sterilization rates using the UV and Gd-doped nano-TiO$_2$ are shown in Fig. 4. The introduction of Gd could also increase the inactivation rate, but the improvement was less obvious. The logarithmic sterilization rates of *Escherichia coli* and *Enterococci* using the

UV and Gd-doped nano-TiO$_2$ treatment (1% Gd content) were 0.735 and 0.720, respectively, which were only 0.086 and 0.094 higher than the UV and nano-TiO$_2$ treatment.

Under UV radiation, electrons of TiO$_2$ photocatalyst could be excited from valence band to conduction band, and electron/hole pairs then move to material surface and initiate the generation of reactive oxygenated species, resulting in the inactivation of bacterial cells. The high degree of recombination between photo-induced electrons and holes is a key restricting factor on the photocatalytic efficiency, and metal doping proved to be an effective way to solve the problem. In this study, the perfect inactivation effect of the UV and Ag-doped nano-TiO$_2$ might be mainly due to the improvement effort of Ag in nano-TiO$_2$. Many studies have proved that Ag could capture photo-generated electrons, inhibit the recombination of electrons and holes, and generate more hydroxyl radicals for inactivation (Bahadur et al. 2016; Rtimi et al. 2019). With high concentrations of reactive oxygenated species, phospholipid peroxidation led to significant breakdown of bacterial membrane structure and inhibition of bacterial DNA replication, resulting in the death of bacteria. Moreover, it has been reported that the Ag-TiO$_2$ nanoparticles had better antibacterial activity through theoretical quantum chemical calculation and electronic analysis

Fig. 5 SEM images of the four kinds of materials. **a** Nano-TiO$_2$, **b** 1% Ag-doped nano-TiO$_2$, **c** 1% Fe-doped nano-TiO$_2$, and **d** 1% Gd-doped nano-TiO$_2$
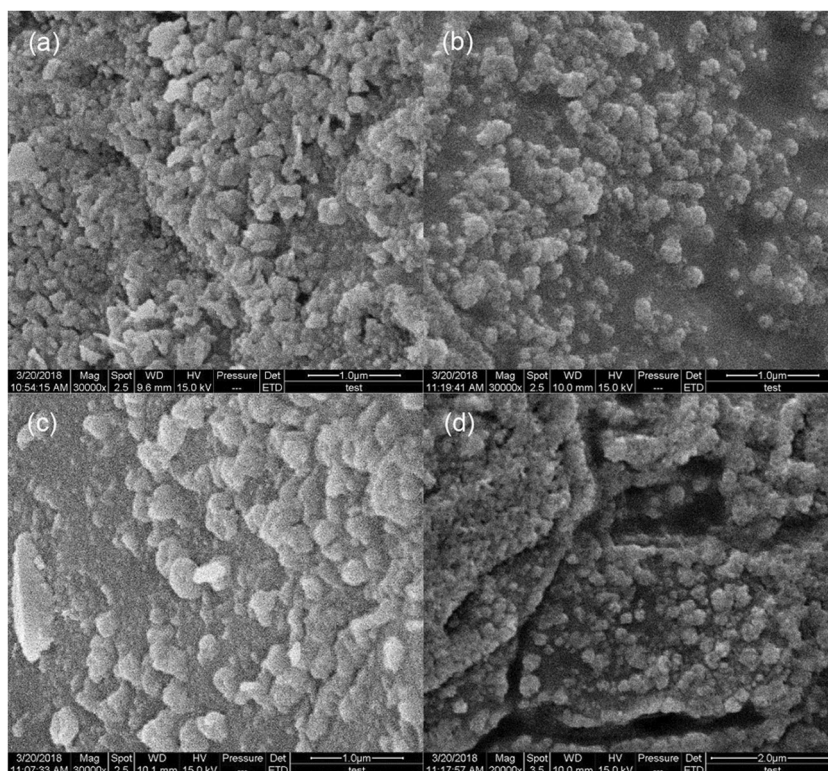
(André et al. 2015). Based on the results, the doping of Ag was an effective strategy to improve the inactivation effect of the UV and nano-TiO$_2$ treatment.

Experimental results indicate that the doping of Fe could also improve the sterilization effect of nano-TiO$_2$. Previous study has reported that the Fe-TiO$_2$ film has better photocatalytic effect than the sole TiO$_2$ (Sun et al. 2009). Since Fe and Ti are of the very similar ionic radius, Fe in the TiO$_2$ film could replace Ti in the lattice, resulting in efficient separation and recombination of photo-generated electrons and holes (Sun et al. 2009, Wang et al. 2003). For the doping of Gd, the insignificant improvement might be because the doping of Gd could simultaneously cause positive and negative efforts on TiO$_2$ photocatalysis. On the positive aspects, the incorporation of Gd into TiO$_2$ could shorten the charge transfer distance (Reddy et al. 2001). The doping of Gd also helps to transfer light-induced charge carriers to surface-adsorbed materials, improving photocatalytic activity by enhancing the electronic band structure and light response. On the opposite, the ionic radius of Gd is larger than Ti, so that Gd locates in the interstitial position and induces a stress in the matrix (Baiju et al. 2010). Hence, Gd might not be suitable as the additive of the nano-TiO$_2$ for bacterial inactivation.

Microstructure and composition of the Ag, Fe, and Gd-doped nano-TiO$_2$

Microstructure of the original nano-TiO$_2$, 1% Ag-doped nano-TiO$_2$, 1% Fe-doped nano-TiO$_2$, and 1% Gd-doped nano-TiO$_2$ was analyzed by SEM analysis (Fig. 5). It indicates that the doping of Ag, Fe, and Gd prevented the aggregation of nanoparticles on the surface of the material. Among the four materials, the microstructure of 1% Ag-doped nano-TiO$_2$ showed the smallest particle diameter and the evenest distribution of the nanoparticles, which was in consistent with the preferable inactivation effort in this case. For 1% Ag-doped nano-TiO$_2$, the smallest grain size after doping meant the largest specific surface area for photocatalysis. Under the UV radiation, there were more photocatalysis sites on the material surface. More reactive oxygenated species could be induced for 1% Ag-doped nano-TiO$_2$, causing the deconstruction of the bacterial cell wall and plasma membrane, the leakage of cellular contents, and then cell death (Allahverdiyev et al. 2011; Li et al. 2012; Yang et al. 2013).

The composition of the original nano-TiO$_2$, 1% Ag-doped nano-TiO$_2$, 1% Fe-doped nano-TiO$_2$, and 1% Gd-doped nano-TiO$_2$ was determined by the EDS analysis (Fig. 6). It indicates that small amounts of Ag, Fe, and Gd were separately doped into the original nano-TiO$_2$. For the four materials, the crystal morphology and phase
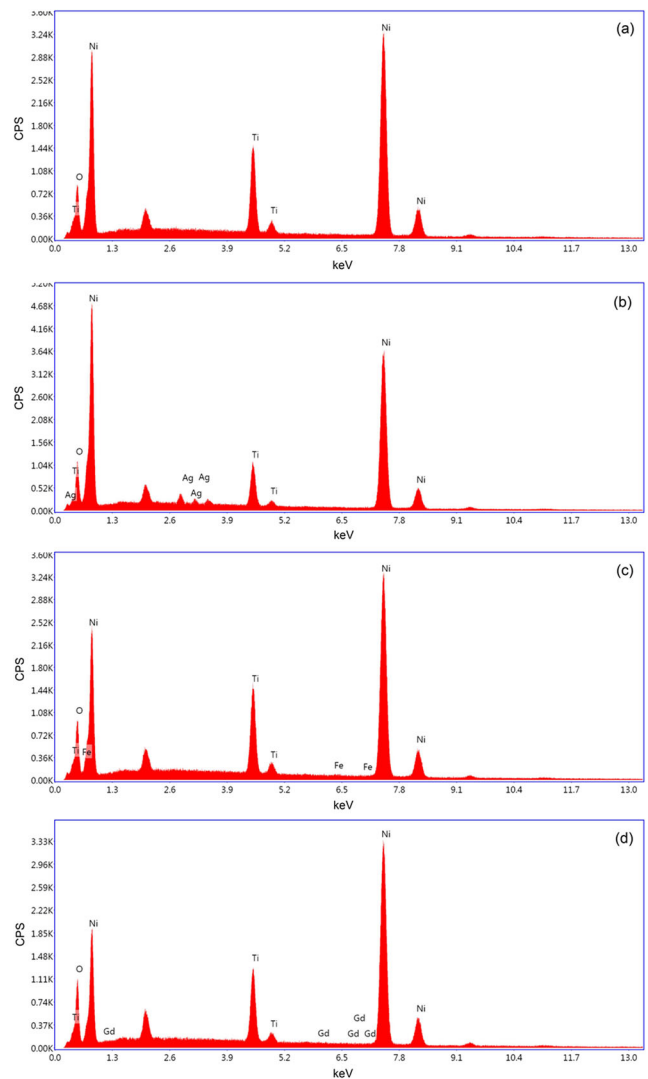
Fig. 6 EDS images of the four kinds of materials. **a** Nano-TiO$_2$, **b** 1% Ag-doped nano-TiO$_2$, **c** 1% Fe-doped nano-TiO$_2$, and **d** 1% Gd-doped nano-TiO$_2$

were analyzed by the XRD analysis (Fig. 7). These samples all corresponded to the crystal structure of anatase TiO$_2$ (JCPDS 01-084-1285) (Durupthy et al. 2007). The average particle diameters of the original nano-TiO$_2$, 1% Ag-doped nano-TiO$_2$, 1% Fe-doped nano-TiO$_2$, and 1% Gd-doped nano-TiO$_2$ were calculated by Scherrer's formula to be 18 nm, 11 nm, 13 nm, and 15 nm, respectively. The antibacterial activity of nano-TiO$_2$ is closely related to its crystal state, and the anatase phase TiO$_2$ can exert better catalytic effect than rutile and amorphous TiO$_2$ (Xue et al. 2013). The doping of Ag, Fe, and Gd did not change the crystal form of the anatase phase but decreased the grain size to varying degrees. The increased specific surface area might be a key reason for the improvement of photocatalytic inactivation effect.

Fig. 7 XRD images of the four kinds of materials. **a** Nano-TiO₂, **b** 1% Ag-doped nano-TiO₂, **c** 1% Fe-doped nano-TiO₂, and **d** 1% Gd-doped nano-TiO₂
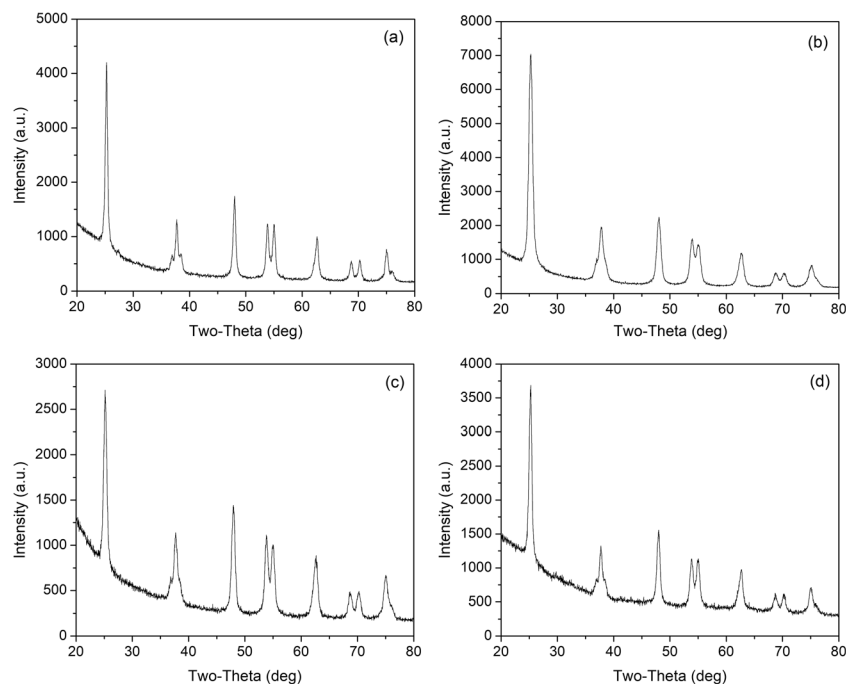
## MDA content and SOD activity during the inactivation process

Under harsh environments, a large amount of reactive oxygenated species is accumulated in the cells to generate more active free radicals. Cell membrane undergoes lipid peroxide reaction to form MDA, which is considered a good indicator to reflect the degree of damage to the microbial cells (Mateos et al. 2005). For *Escherichia coli* and *Enterococci*, Fig. 8 shows MDA concentrations under the treatment of the sole UV and the UV and Ag-doped nano-TiO₂. Compared with the approximate linear increase of MDA content by the sole UV treatment, the MDA concentration increased rapidly under the UV and Ag-doped nano-TiO₂ treatment. At the end of the inactivation process, the MDA concentration under the UV and Ag-doped nano-TiO₂ treatment reached 0.0646 μmol/L for *Escherichia coli* and 0.0529 μmol/L for *Enterococci*, which were about 1.61 times and 1.71 times the values of the sole UV treatment (0.0402 μmol/L for *Escherichia coli* and 0.0309 μmol/L for *Enterococci*), respectively. Since the concentration of MDA can reflect the degree of damage of reactive oxygenated species in cells (Halliwell and Chirico 1993; Onorato et al. 1998), the high MDA contents under the UV and Ag-doped nano-TiO₂ treatment indicate that much more reactive oxygenated species were generated in these cases, leading to high inactivation rates of *Escherichia coli* and *Enterococci*.

As an important antioxidase, SOD scavenges superoxide radicals (O^{2-}) in organisms to protect cells from the damage of free radicals (Huang et al. 2000). SOD activity is a key factor influencing self-repair process within the cells. The SOD activities in *Escherichia coli* and *Enterococcus* under the sole UV treatment and the UV and Ag-doped nano-TiO₂ treatment are shown in Fig. 9. Compared with the sole UV treatment, the SOD activity under the UV and Ag-doped nano-TiO₂ performed a faster decrease trend during the process. At the end of the inactivation process, the SOD activity under the UV and Ag-doped nano-TiO₂ was 0.672 U/mL for *Escherichia coli* and 0.792 U/mL for *Enterococci*, which were significantly lower than those of the sole UV treatment (1.207 U/mL for *Escherichia coli* and 1.187 U/mL for *Enterococci*). With low SOD activities, normal cell metabolism of *Escherichia coli* and *Enterococci* was greatly inhibited by a large number of reactive oxygenated species generated during the UV and Ag-doped nano-TiO₂ treatment. The accumulation of reactive oxygenated species accelerated the deconstruction of bacterial cell structure and then led to the death of bacteria. The results indicate that the UV and Ag-doped nano-TiO₂ treatment surely has more remarkable inactivation effect than the sole UV treatment.
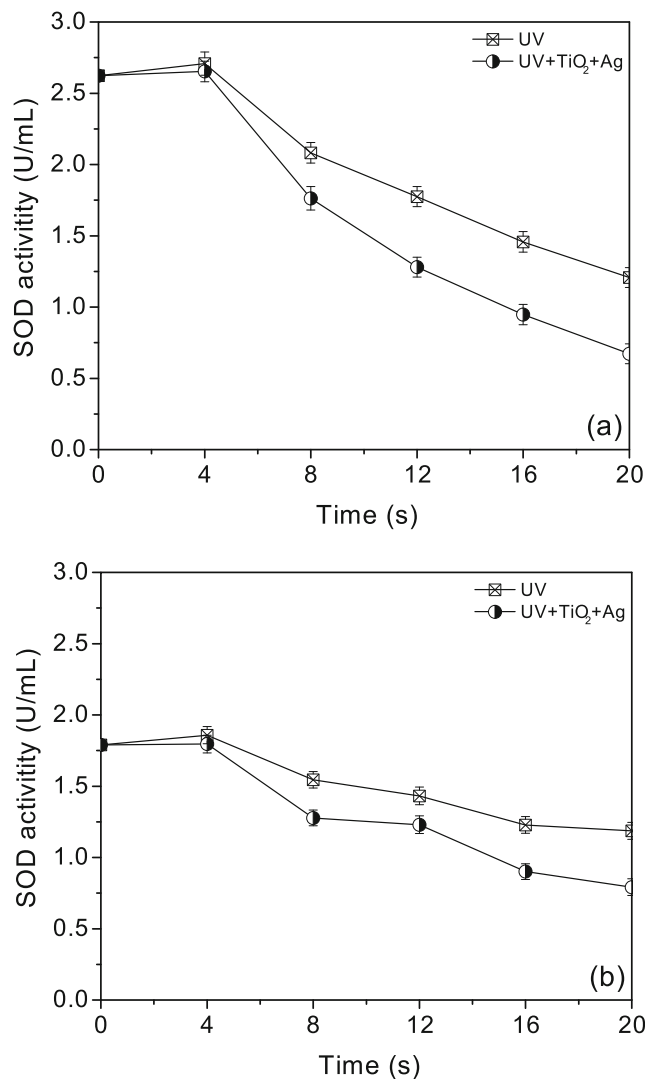
Conclusions

To improve bacterial inactivation effect for ship ballast water treatment, Ag, Fe, and Gd were doped to nano-TiO₂ at different ratios (0.4%, 0.7%, and 1.0%) to prepare
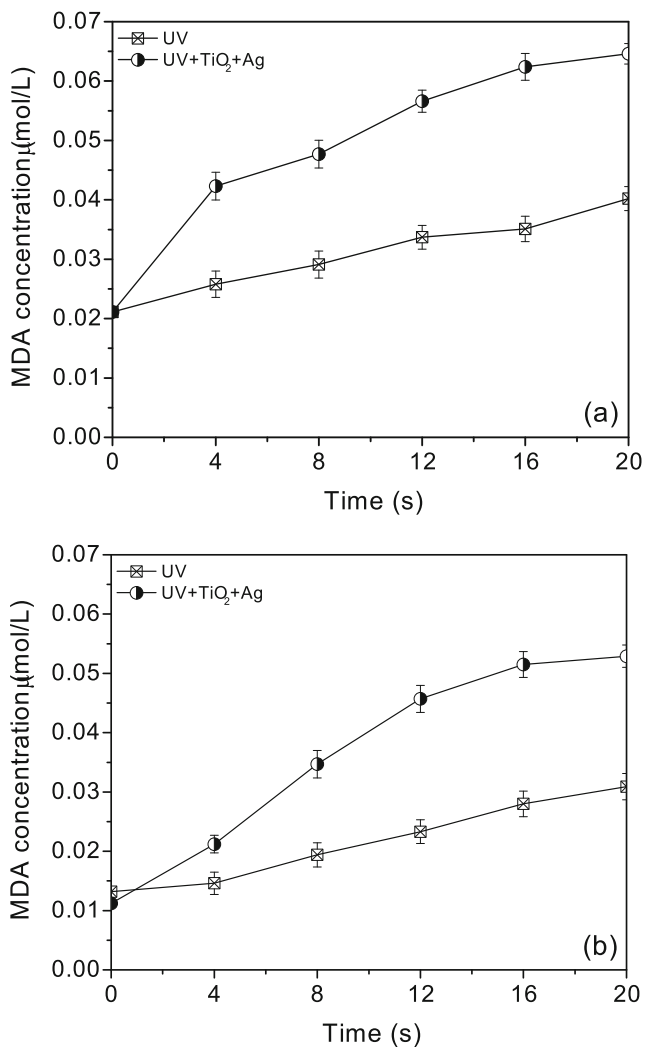
Fig. 8 MDA concentration under the treatment of the sole UV and the UV and Ag-doped nano-TiO₂. **a** *Escherichia coli* and **b** *Enterococci*

Fig. 9 SOD activity under the treatment of the sole UV and the UV and Ag-doped nano-TiO₂. **a** *Escherichia coli* and **b** *Enterococci*

metal-doped nano-TiO$_2$. Compared with the sole UV and the UV and nano-TiO$_2$, the UV and metal-doped nano-TiO$_2$ increased the inactivation rate of *Escherichia coli* and *Enterococci* to different extents. For each metal, high external metal content (1.0%) corresponded to high inactivation effort. Among the three metal elements, the doping of Ag resulted in the optimal inactivation effect, and the addition of Fe and Gd caused unobvious efforts. At the treatment time of 20 s, the UV and 1% Ag-doped nano-TiO$_2$ reached the highest logarithmic sterilization rates of *Escherichia coli* and *Enterococcus* with the values of 0.915 and 0.805, respectively. SEM and XRD analysis indicate that the doping of Ag, Fe, and Gd did not change the anatase phase TiO$_2$ crystal form and the microstructure of 1% Ag-doped nano-TiO$_2$ performed the smallest particle diameter and the evenest distribution of nanoparticles. Compared with the sole UV treatment, the

UV and Ag-doped nano-TiO$_2$ treatment resulted in higher MDA contents (0.0646 μmol/L for *Escherichia coli* and 0.0529 μmol/L for *Enterococci*) and lower SOD activities (0.672 U/mL for *Escherichia coli* and 0.792 U/mL for *Enterococci*), which provides theoretical explanation for high inactivation rates in these cases.

Compliance with ethical standards

Conflict of interest The authors declare that they have no conflict of interest.

References

Allahverdiyev AM, Abamor ES, Bagirova M, Ustundag CB, Kaya C, Kaya F, Rafailovich M (2011) Antileishmanial effect of silver nanoparticles and their enhanced antiparasitic activity under ultraviolet light. Int J Nanomedicine 6:2705–2714

André RS, Zamperini CA, Mima EG, Longo VM, Albuquerque AR, Sambrano JR, Machado AL, Vergani CE, Hernandes AC, Varela JA, Longo E (2015) Antimicrobial activity of TiO_2: Ag nanocrystalline heterostructures: experimental and theoretical insights. Chem Phys 459:87–95

Bahadur J, Agrawal S, Panwar V, Parveen A, Pal K (2016) Antibacterial properties of silver doped TiO_2 nanoparticles synthesized via sol-gel technique. Macromol Res 24:488–493

Baiju KV, Periyat P, Shajesh P, Wunderlich W, Manjumol KA, Smitha VS, Jaimy KB, Warrier KGK (2010) Mesoporous gadolinium doped titania photocatalyst through an aqueous sol gel method. J Alloys Compd 505:194–200

Banerjee AN, Hamnabard N, Joo SW (2016) A comparative study of the effect of Pd-doping on the structural, optical, and photocatalytic properties of sol–gel derived anatase TiO_2 nanoparticles. Ceram Int 42:12010–12026

Durupthy O, Bill J, Aldinger F (2007) Bioinspired synthesis of crystalline TiO_2: effect of amino acids on nanoparticles structure and shape. Cryst Growth Des 7:2696–2704

Esterbauer H (1996) Estimation of peroxidative damage. A critical review. Pathol Biol 44:25–28

Halliwell B, Chirico S (1993) Lipid peroxidation: its mechanism, measurement, and significance. Am J Clin Nutr 57(5):715S–724S

Huang P, Feng L, Oldham EA, Keating MJ, Plunkett W (2000) Superoxide dismutase as a target for the selective killing of cancer cells. Nature 407:390–395

Leichsenring J, Lawrence J (2011) Effect of mid-oceanic ballast water exchange on virus-like particle abundance during two trans-pacific voyages. Mar Pollut Bull 62:1103–1108

Li Y, Zhang W, Niu J, Chen Y (2012) Mechanism of photogenerated reactive oxygen species and correlation with the antibacterial properties of engineered metal-oxide nanoparticles. ACS Nano 6:5164–5173

Lu Z, Zhang K, Shi Y, Huang Y, Wang X (2018) Efficient removal of *Escherichia coli* from ballast water using a combined high-gradient magnetic separation-ultraviolet photocatalysis (HGMS-UV/TiO_2) system. Water Air Soil Pollut 229:243

Lu Z, Zhang K, Liu X, Shi Y (2019) High efficiency inactivation of microalgae in ballast water by a new proposed dual-wave UV-photocatalysis system (UVA/UVC-TiO_2). Environ Sci Pollut Res 26:7785–7792

Makropoulou T, Panagiotopoulou P, Venieri D (2018) N-doped TiO_2 photocatalysts for bacterial inactivation in water. J Chem Technol Biotechnol 93:2518–2526

Mamlook R, Badran O, Abu-Khader MM, Holdo A, Dales J (2008) Fuzzy sets analysis for ballast water treatment systems: best available control technology. Clean Technol Environ 10:397–407

Mangayayam M, Kiwi J, Giannakis S, Pulgarin C, Zivkovic I, Magrez A, Rtimi S (2017) FeOx magnetization enhancing *E. coli* inactivation by orders of magnitude on Ag-TiO_2 nanotubes under sunlight. Appl Catal B Environ 202:438–445

Marklund S, Marklund G (1974) Involvement of the superoxide anion radical in the autoxidation of pyrogallol and a convenient assay for superoxide dismutase. Eur J Biochem 47:469–474

Martínez LF, Mahamud MM, Lavín AG, Bueno JL (2013) The regrowth of phytoplankton cultures after UV disinfection. Mar Pollut Bull 67: 152–157

Mateos R, Lecumberri E, Ramos S, Goya L, Bravo L (2005) Determination of malondialdehyde (MDA) by high-performance liquid chromatography in serum and liver as a biomarker for oxidative stress: application to a rat model for hypercholesterolemia and evaluation of the effect of diets rich in phenolic antioxidants from fruits. J Chromatogr B 827:76–82

Milosevic I, Jayaprakash A, Greenwood B, van Driel B, Rtimi S, Bowen P (2017) Synergistic effect of fluorinated and N doped TiO_2 nanoparticles leading to different microstructure and enhanced photocatalytic bacterial inactivation. Nanomater 7:391

Onorato JM, Thorpe SR, Baynes JW (1998) Immunohistochemical and ELISA assays for biomarkers of oxidative stress in aging and disease. Ann N Y Acad Sci 854:277–290

Radzig M, Koksharova O, Khmel I, Ivanov V, Yorov K, Kiwi J, Rtimi S, Tastekova E, Aybush A, Nadtochenko V (2019) Femtosecond spectroscopy of Au hot-electron injection into TiO_2: evidence for Au/TiO_2 plasmon photocatalysis by bactericidal Au ions and related phenomena. Nanomater 9:217

Reddy BM, Chowdhury B, Smirniotis PG (2001) An XPS study of La_2O_3 and In_2O_3 influence on the physicochemical properties of MoO_3/TiO_2 catalysts. Appl Catal A Gen 219:53–60

Roy B, Chandrasekaran H, Krishnan SP, Chandrasekaran N, Mukherjee A (2018) UV A pre-irradiation to P25 titanium dioxide nanoparticles enhanced its toxicity towards freshwater algae Scenedesmus obliquus. Environ Sci Pollut Res 25:1–14

Rtimi S, Dionysiou DD, Pillai SC, Kiwi J (2019) Advances in catalytic/photocatalytic bacterial inactivation by nano Ag and Cu coated surfaces and medical devices. Appl Catal B Environ 240:291–318

Seiden JM, Way C, Rivkin RB (2010) Microbial hitchhikers: dynamics of bacterial populations in ballast water during a trans-Pacific voyage of a bulk carrier. Aquat Invasions 5:13–22

Shang C, Cheung LM, Ho C, Zeng M (2009) Repression of photoreactivation and dark repair of coliform bacteria by TiO_2-modified UV-C disinfection. Appl Catal B Environ 89:536–542

Smirnova N, Petrik I, Vorobets V, Kolbasov G, Eremenko A (2017) Sol-gel synthesis, photo- and electrocatalytic properties of mesoporous TiO_2 modified with transition metal ions. Nanoscale Res Lett 12(1): 239

Sun L, Li J, Wang CL, Li SF, Chen HB, Lin CJ (2009) An electrochemical strategy of doping Fe^{3+} into TiO_2 nanotube array films for enhancement in photocatalytic activity. Sol Energ Mater Sol Cells 93: 1875–1880

Tang Z, Butkus MA, Xie YF (2009) Enhanced performance of crumb rubber filtration for ballast water treatment. Chemosphere 74:1396–1399

Tao P, Xu Y, Zhou Y, Song C, Shao M, Wang T (2017) Coal-based carbon membrane coupled with electrochemical oxidation process for the enhanced microalgae removal from simulated ballast water. Water Air Soil Pollut 228(11):421

Tsolaki E, Diamadopoulos E (2010) Technologies for ballast water treatment: a review. J Chem Technol Biotechnol 85:19–32

Veziroglu S, Ghori MZ, Kamp M, Kienle L, Rubahn HG, Strunskus T, Fiutowski J, Adam J, Faupel F, Aktas OC (2018) Photocatalytic growth of hierarchical au needle clusters on highly active TiO_2 thin film. Adv Mater Interfaces 5(15):1800465

Wang C, Böttcher C, Bahnemann DW, Dohrmann JK (2003) A comparative study of nanometer sized Fe(iii)-doped TiO_2 photocatalysts: synthesis, characterization and activity. J Mater Chem 13:2322–2329

Wu M, Wu P, Lin T, Lin T (2018) Photocatalytic performance of Cu-doped TiO_2 nanofibers treated by the hydrothermal synthesis and air-thermal treatment. Appl Surf Sci 430:390–398

Xue X, Wang Y, Yang H (2013) Preparation and characterization of boron-doped titania nano-materials with antibacterial activity. Appl Surf Sci 264:94–99

Yang L, Wen Z, Junfeng N, Yongsheng C (2013) Surface-coating-dependent dissolution, aggregation, and reactive oxygen species

(ROS) generation of silver nanoparticles under different irradiation conditions. Environ Sci Technol 47(18):10293–10301

Yang M, Weiqu L, Chi J, Sha H, Yankun X, Zhengfang W (2018) Fabrication of superhydrophobic cotton fabric with fluorinated TiO_2 sol by a green and one-step sol-gel process. Carbohydr Polym 197:75–82

Yu J, Wang T, Rtimi S (2019) Magnetically separable TiO_2/FeOx/POM accelerating the photocatalytic removal of the emerging endocrine disruptor: 2,4-dichlorophenol. Appl Catal B Environ 254:66–75